Various consequences of disorder on strongly correlated systems

D.D. Sarma

Solid State and Structural Chemistry Unit

Indian Institute of Science

Bangalore

sarma@sscu.iisc.ernt.in

http://sscu.iisc.ernet.in/DDSarma/

- Sugata Ray
- Dinesh Topwal
- Manju Unnikrishnan
- Prabuddha Sanyal
- Subhra Sengupta
- Priya Mahadevan
- Tanusri Saha-Dasgupta

- H.R. Krishnamurthy
- Chandan Dasgupta
- E. V. Sampathkumaran
- A. Fujimori
- Y. Tokura
- C. Meneghini
- C. Segre
- D. Matsumura and T. Ohta

Department of Science and Technology, Government of India

Sr_2FeMoO_6 - a compound with many faces

In general $A_2BB'O_6$ 

Ordered Double Perovskite

Is it $ABO_3 + AB'O_3$?

Sr_2FeMoO_6 :
$Sr_2Fe_{1-x}Mo_{1+x}O_6$
($SrFeO_3/SrMoO_3$),
$Sr_2FeMo_{1-x}W_xO_6$
(Sr_2FeMoO_6/Sr_2FeWO_6)

$Mn_xGa_{1-x}As$ and $Tl_2Mn_2O_7$

Some typical publications in this field from our group

- **Phys. Rev. Lett. (in press 2009).**
- **Phys. Rev. Lett. 100, 186402 (2008).**
- **Phys. Rev. Lett. 98, 246401 (2007).**
- **Phys. Rev. Lett. 98, 157205 (2007).**
- **Phys. Rev. Lett. 96, 087205 (2006)**
- **Phys. Rev. Lett. 95, 117201 (2005).**
- **Nano Lett. 2, 605 (2002).**
- **Phys. Rev. Lett. 87, 097204 (2001).**
- **Phys. Rev. Lett. 85, 2549 (2000).**
- **Solid State Comm. 114, 465 (2000).**

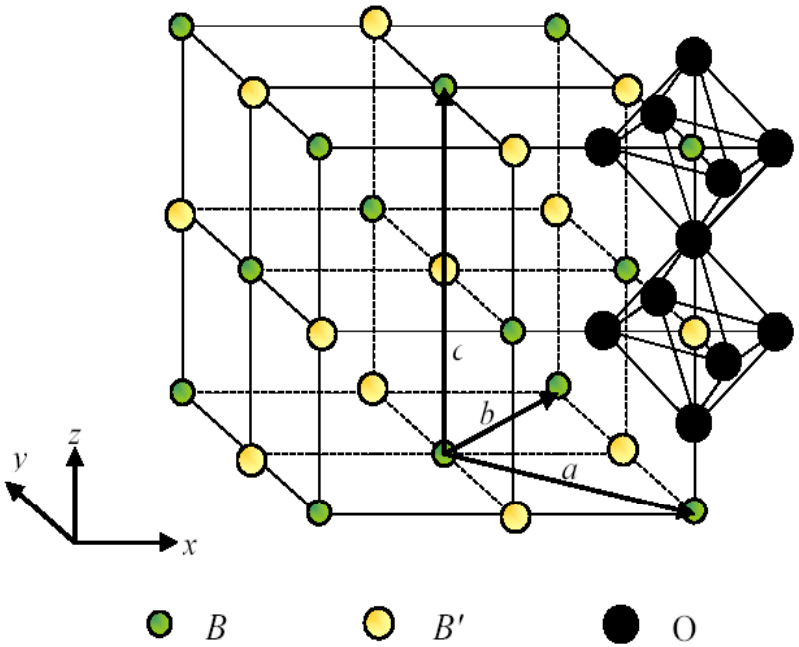

Crystal structure of **ordered** double **perovskite**: $A_2BB'O_6$

Sr Fe Mo O

D.D.Sarma, Current Opinion in Solid State and Materials Science (2001)

and

Phys. Rev. Lett. 85, 2549 (2000).

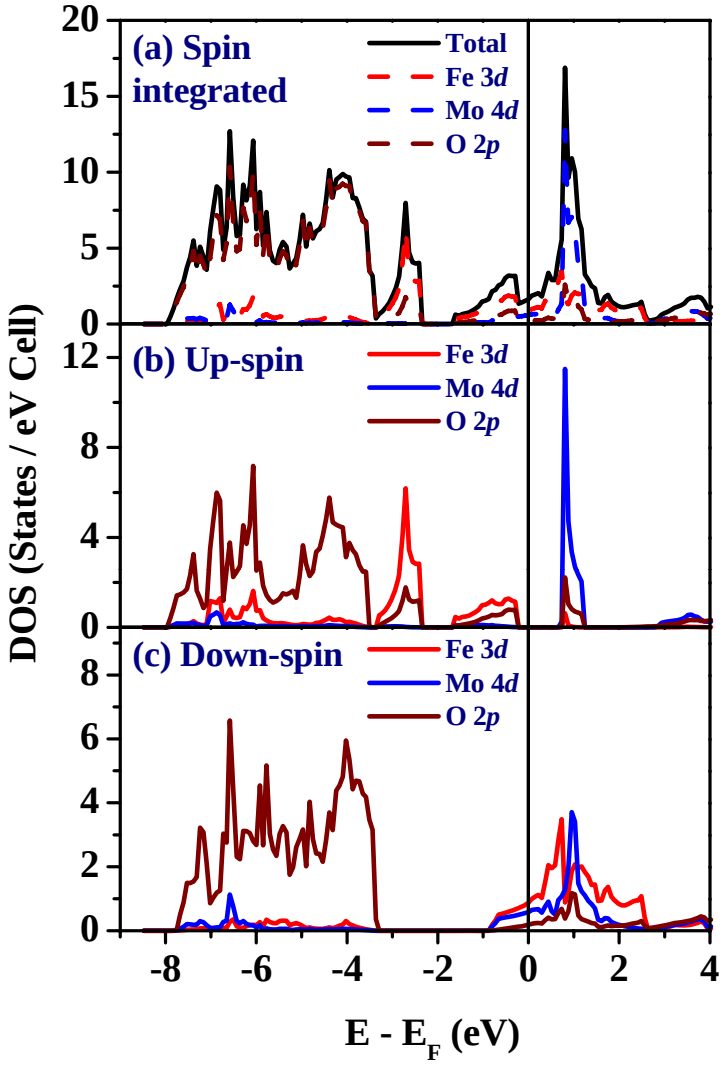

LMTO band structure results of Sr_2FeMoO_6

Magnetoresistance in polycrystalline Sr_2FeMoO_6

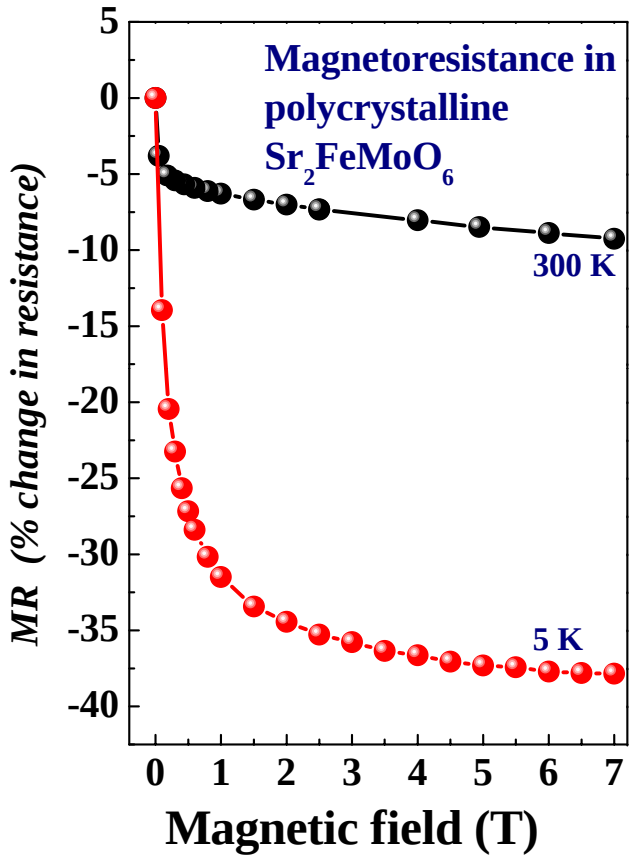

Sarma et al., Solid State Comm. 114, 465 (2000).

Several advantages:

- Large MR at higher T and lower H.
- High ferromagnetic T_c.
- Half-metallic ferromagnet (100% spin polarization of charge carriers).
- Simple crystal structure. Possibly, no serious complication arising from J-T type distortions.

Therefore, attractive both in terms of theoretical investigations and possible technological applications.

On the basis of the structural data, however, ferromagnetism appears to be a rather unexpected ground state for this system.

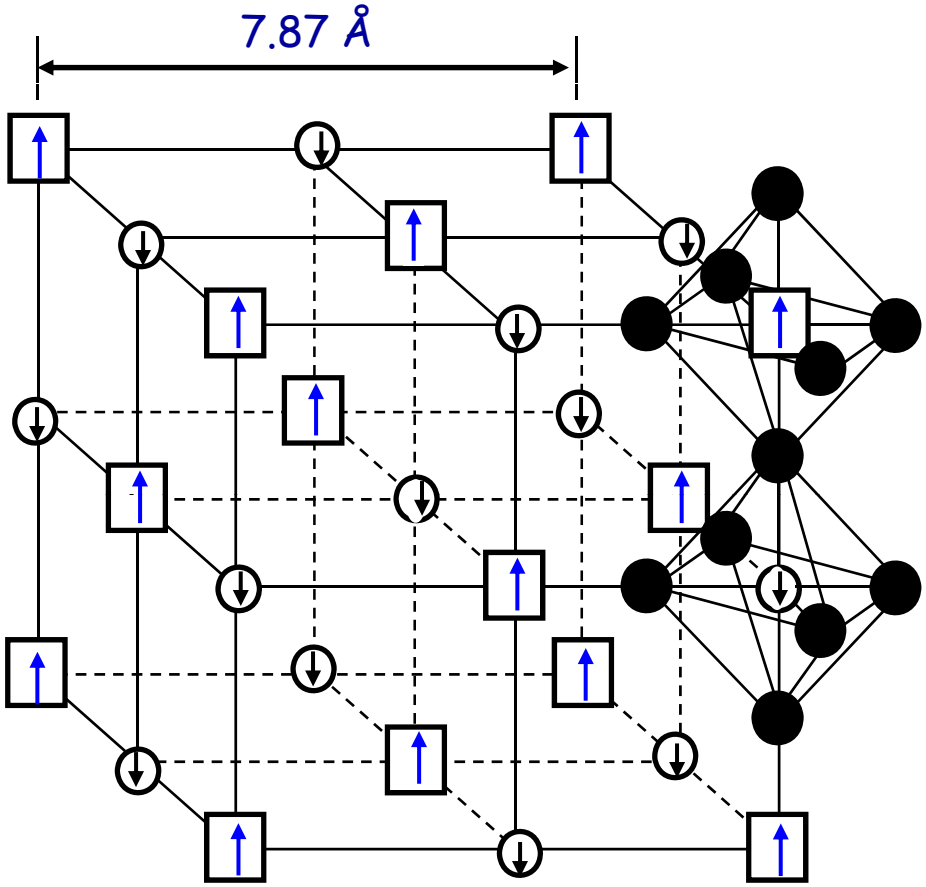

Fe

$3d^5$

$S = 5/2$

Mo

Usually non-magnetic, nominally $4d^1$ $S = 1/2$

O

Nonmagnetic

T_C = 420 K

Weak AF interaction between Fe ions, governed by super-exchange, is expected and also found in Sr_2FeWO_6

What is the origin of the strong ferromagnetic interaction between Fe ions in this compound, implicit in such an unusually high T_C?

Superexchange between Fe up- and Mo down-spins?

Or double-exchange?

Must be a different mechanism from the manganites that polarises the delocalised, nominally Mo derived, conduction electrons.

Origin of the robust ferromagnetism in double perovskite, Sr_2FeMoO_6

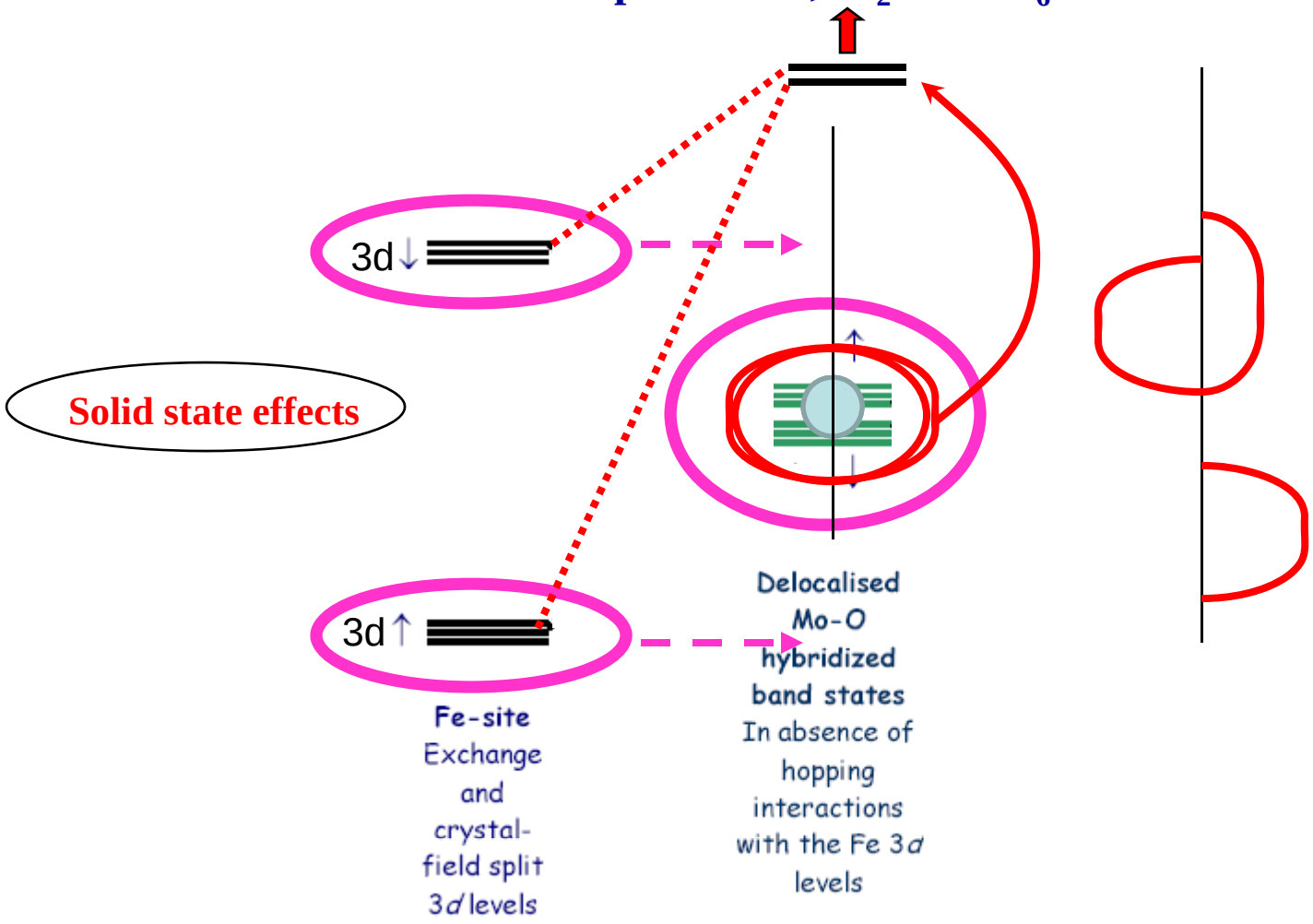

Intra-atomic, I_{eff} ~ 1-1.5 eV, Inter-atomic, J ~ 18 meV

Why Sr_2FeWO_6 is an antiferromagnet?

Sarma et al., PRL 85, 2549 (2000).

Hopping induced antiferromagnetic coupling of itinerant and localized spins ⟹ Ferromagnetic coupling of the localized moments.

Half-metallic or not depends on the strength of hopping and other details.

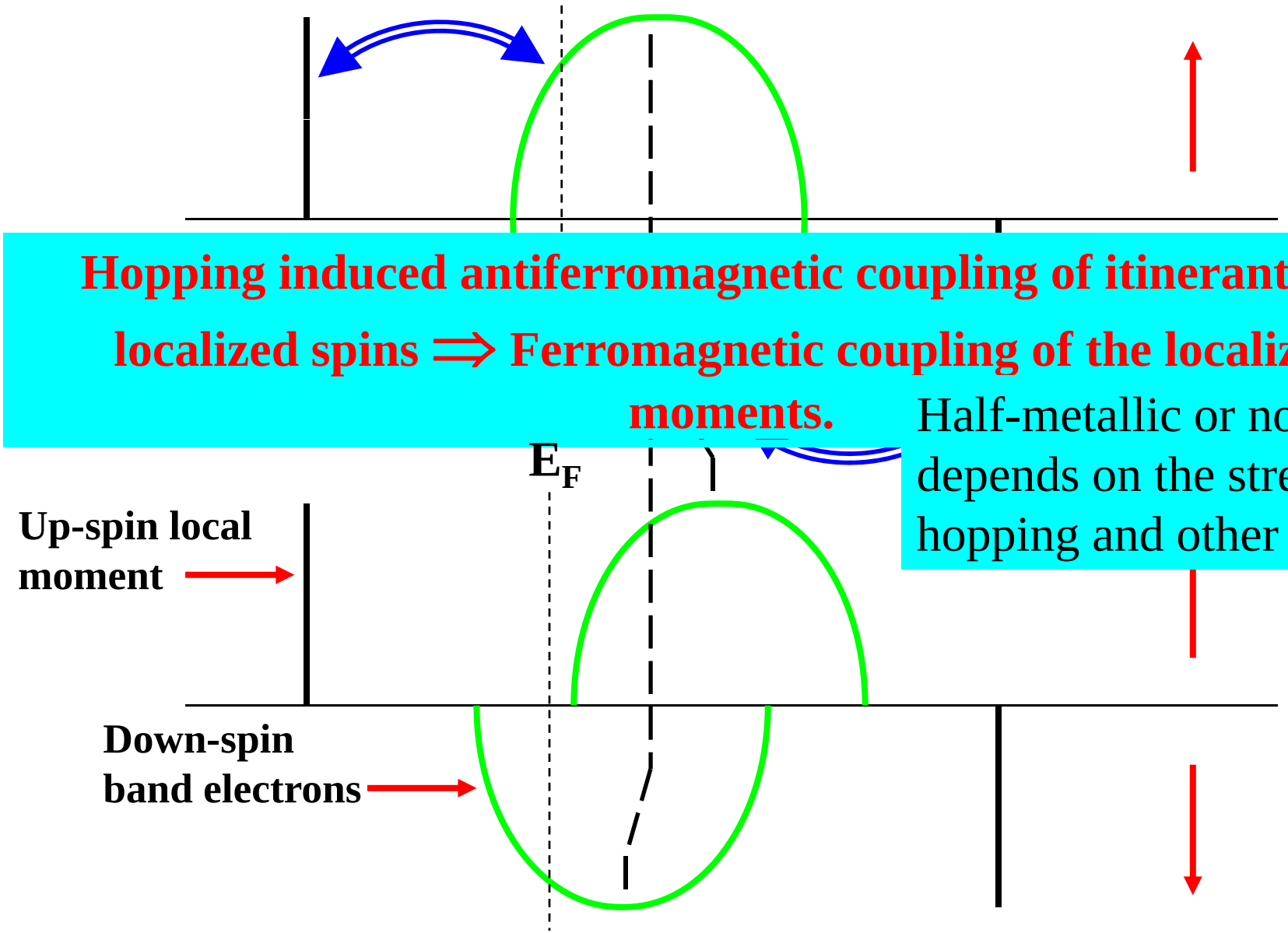

Low doping:

Can be localized by disorder, when the doping level is low, but will remain ferromagnetic!

What about insulating ferromagnetic state in presence of a high carrier density?

Can be localized (structural distortions/electron correlations), but will remain ferromagnetic!

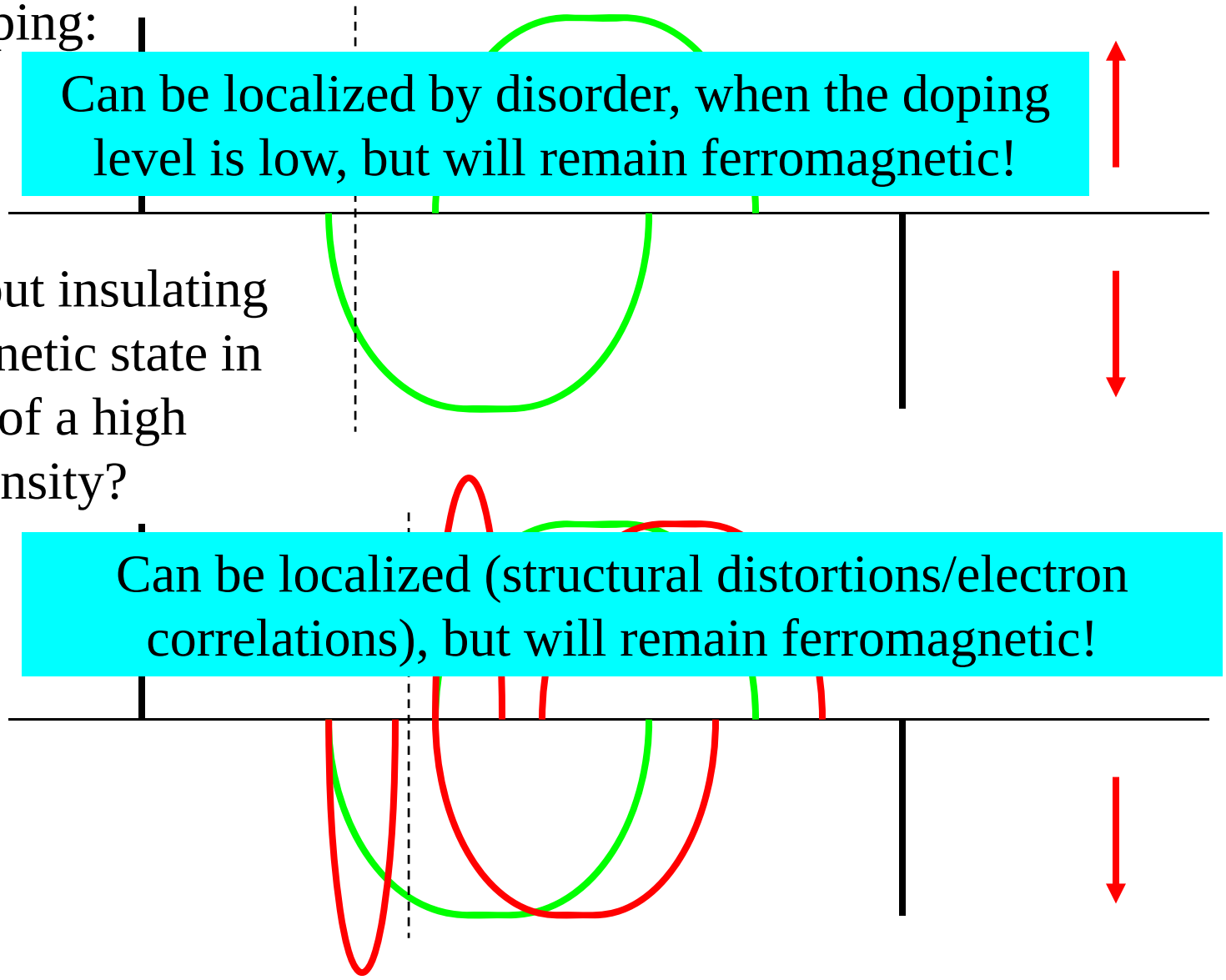

Magnetism in

$Mn_xGa_{1-x}As$: Mahadevan, Zunger and Sarma,

Phys. Rev. Lett. 93, 177201 (2004).

$Tl_2Mn_2O_7$: Saha-Dasgupta, De Raychaudhury and Sarma,

Phys. Rev. Lett. 96, 087205 (2006).

Origin of the ferromagnetism in Mn-doped GaAs

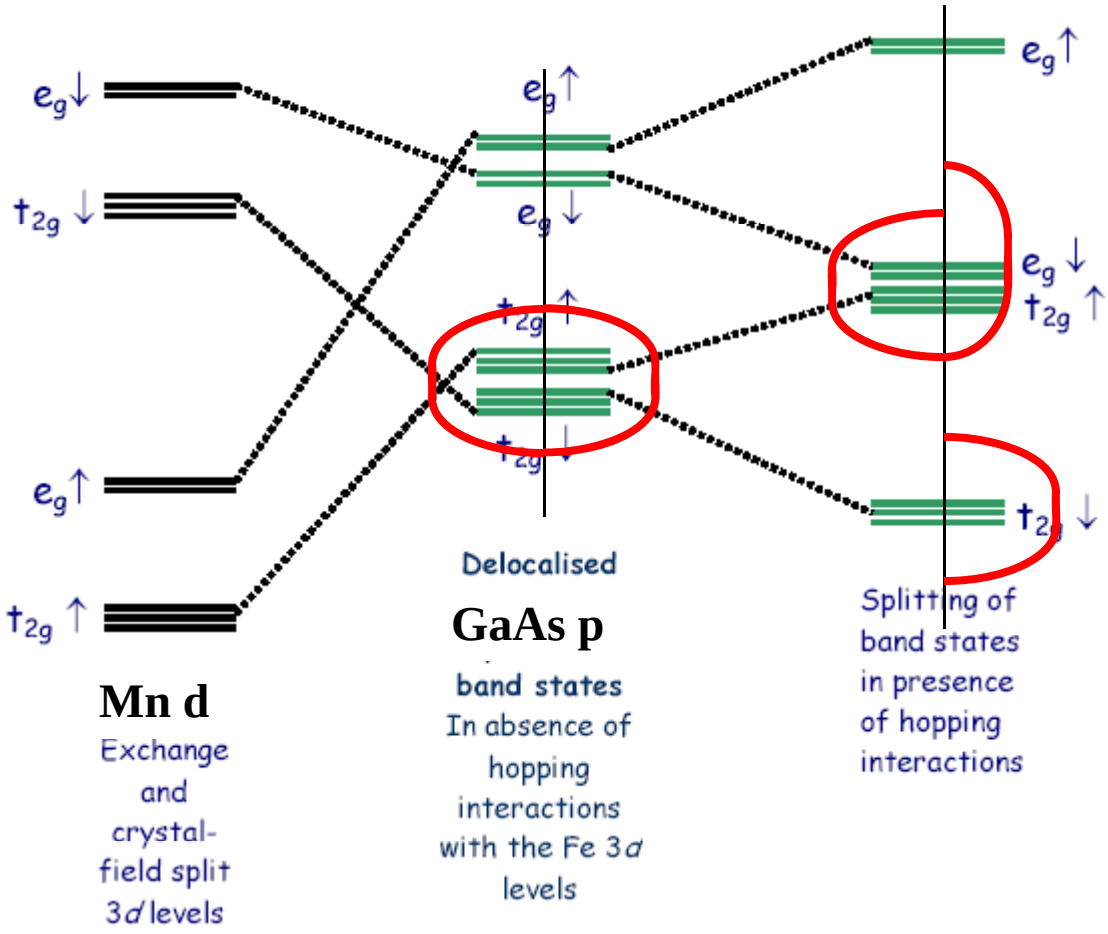

Ferromagnetism in Mn-doped GaAs

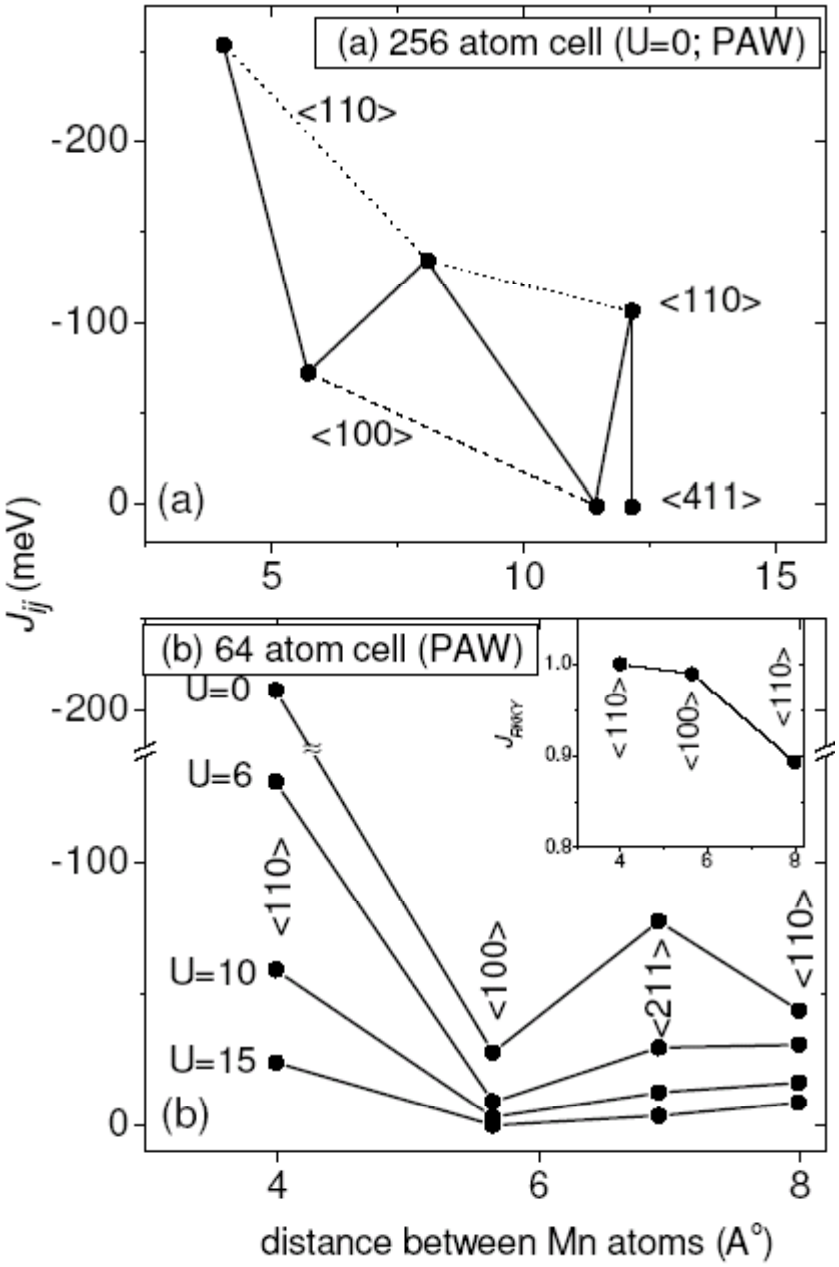

FIG. 4: The distance/orientation dependence of Jij for Mn pairs in (a) 256, (b) 64 atom GaAs cell using PAW potentials. The expected dependence of J_{RKKY} for a hole in GaAs is given in the insert.

Mahadevan, Zunger and Sarma, Phys. Rev. Lett. 93, 177201 (2004).

nature Vol 442|27 July 2006|doi:10.1038/nature04971

LETTERS

Atom-by-atom substitution of Mn in GaAs and visualization of their hole-mediated interactions

Dale Kitchen[1,2], Anthony Richardella[1,2], Jian-Ming Tang[3], Michael E. Flatté[3] & Ali Yazdani[1]

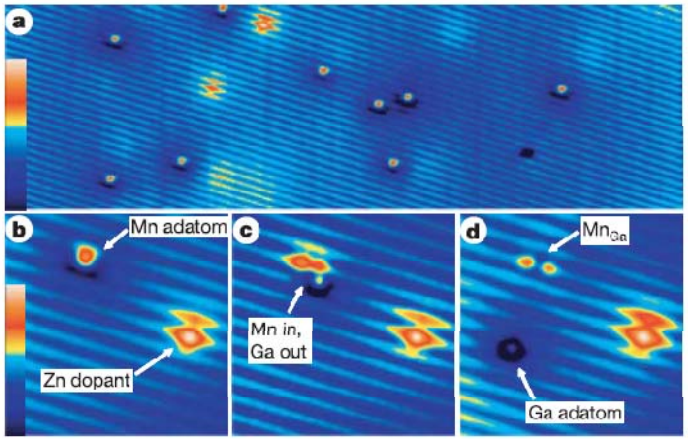

Figure 1 | Single-atom substitution of one Mn for one Ga atom. **a**, Large topograph of the occupied states (500 × 150 Å^2; −2 V; 0–1.5 Å) showing many Mn adsorbates and a few subsurface Zn dopants. **b–d**, High-resolution topographs (75 Å^2; −2 V; 0–1.3 Å). **b**, Mn adsorbate and a Zn acceptor visible on the As sublattice. **c**, STM-assisted incorporation of the Mn into a Ga site forcing the substituted Ga atom to the surface. **d**, Tip-pulses move the Ga adatom from the incorporation site, isolating a Mn acceptor (Mn_{Ga}).

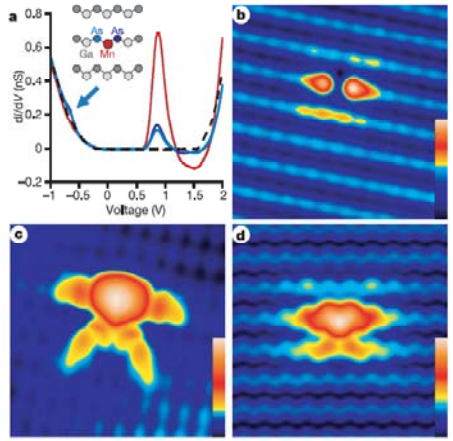

Figure 2 | High-resolution measurements of a single Mn acceptor (Mn_{Ga}). **a**, Spatially resolved d*I*/d*V* measurements near an Mn acceptor. The As neighbours show enhancements deep in the valence band, highlighted by the blue arrow. The large in-gap resonance over the Mn is its acceptor level. **b**, 40 Å^2 topograph of the occupied states (−1.5 V; 0–0.4 Å) showing enhancements concentrated on the neighbouring As. **c**, 40 Å^2 topograph of the unoccupied states (+1.55 V; 0–4 Å) revealing the anisotropic shape of the Mn acceptor. **d**, Tight-binding model of a Mn acceptor in bulk GaAs with the Mn spin oriented in-plane along [001]. The image shows a 40 Å^2 area of the (110) plane containing the Mn. The log of the integrated LDOS from the Fermi level to 1.55 eV is displayed with a spatial broadening factor of 1.7 Å. The colours in the scales have been chosen to enhance the view of the Mn influence on GaAs.

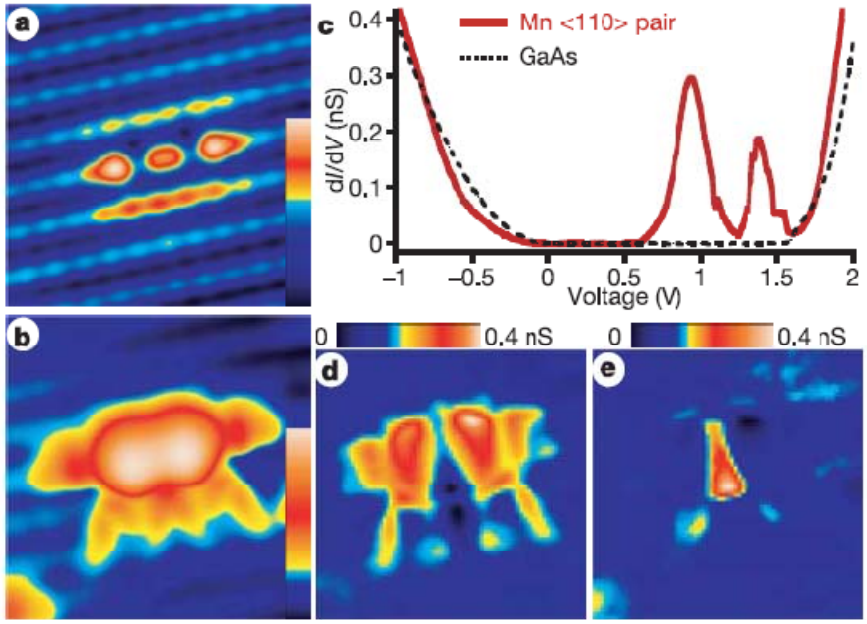

Figure 3 | Mn pair substituted in Ga sites spaced 8 Å apart in a <110> orientation. **a**, 40 Å^2 topograph of the valence-band states (−1.5 V; 0–0.4 Å). **b**, 40 Å^2 topograph of the in-gap states showing the bound states of Mn acceptors (+1.1 V; 0–4 Å). **c**, dI/dV measurements near the Mn pair, revealing two resonance levels in the gap. **d**, Differential conductance energy map at +1.35 V displaying the bonding nature of the higher energy resonance. **e**, Energy map at +0.91 V displaying the anti-bonding nature of the lower energy peak.

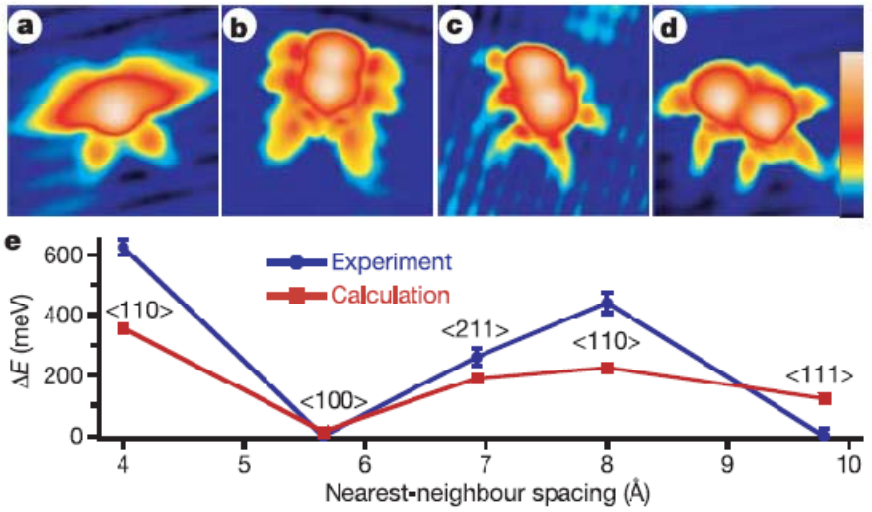

Figure 4 | Topographs (40 Å^2, +1.5 V) of several Mn pairs and the acceptor-level splitting energy of these pairs. **a**, Nearest-neighbour Mn acceptor pair (4 Å spacing, <110> orientation). **b**, Second-nearest-neighbour pair (5.65 Å spacing, <100> orientation). **c**, Third-nearest pair (6.92 Å spacing, <211> orientation). **d**, Sixth-nearest-neighbour pair (9.79 Å spacing, <111> orientation). Figure 3b shows the fourth-nearest-neighbour pair (8 Å spacing, <110> orientation). The fifth-nearest-neighbour is not accessible in a single (110) plane. **e**, Comparative plot of the Mn acceptor-level splitting for Mn–Mn pair interactions. Theory and experiment both show that Mn–Mn interactions are highly anisotropic, favouring <110> orientations. Error bars correspond to the standard deviation of many pairs measured on p-type GaAs (110) surfaces. ΔE, splitting energy of the acceptor levels.

Magnetoresistance in polycrystalline Sr_2FeMoO_6

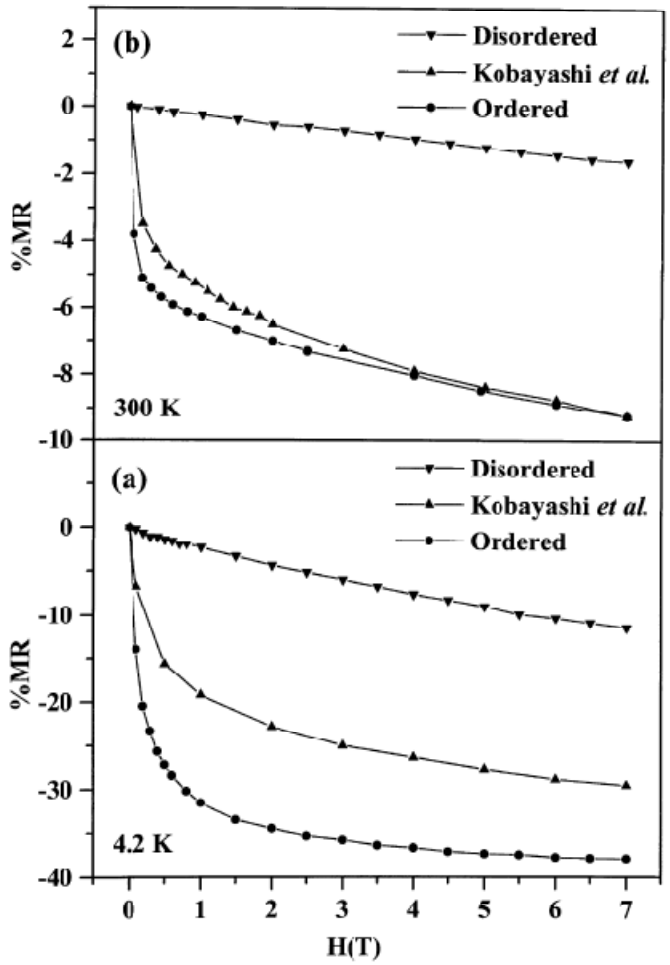

Sarma et al., Solid State Comm. 114, 465 (2000).

But, why does magnetoresistance change so drastically?
Inter- or intra-grain mechanism?

Effect of anti-site disorder in Sr_2FeMoO_6

What is the Fe/Mo antisite disorder?

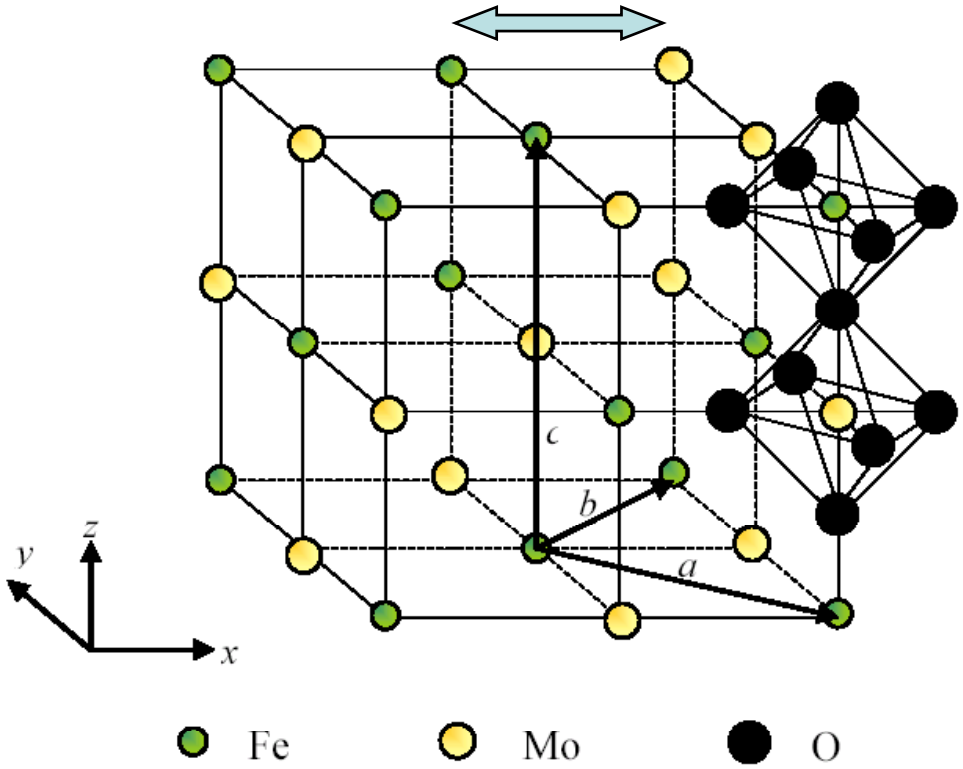

How do we check ordering?

What is the effect of disorder?

Expected magnetic moment: antiparallely aligned Fe^{3+} ($3d^5$; S = 5/2) and Mo^{5+} ($4d^1$; S = ½) = $4\mu_B$ / f.u.

X-ray diffraction

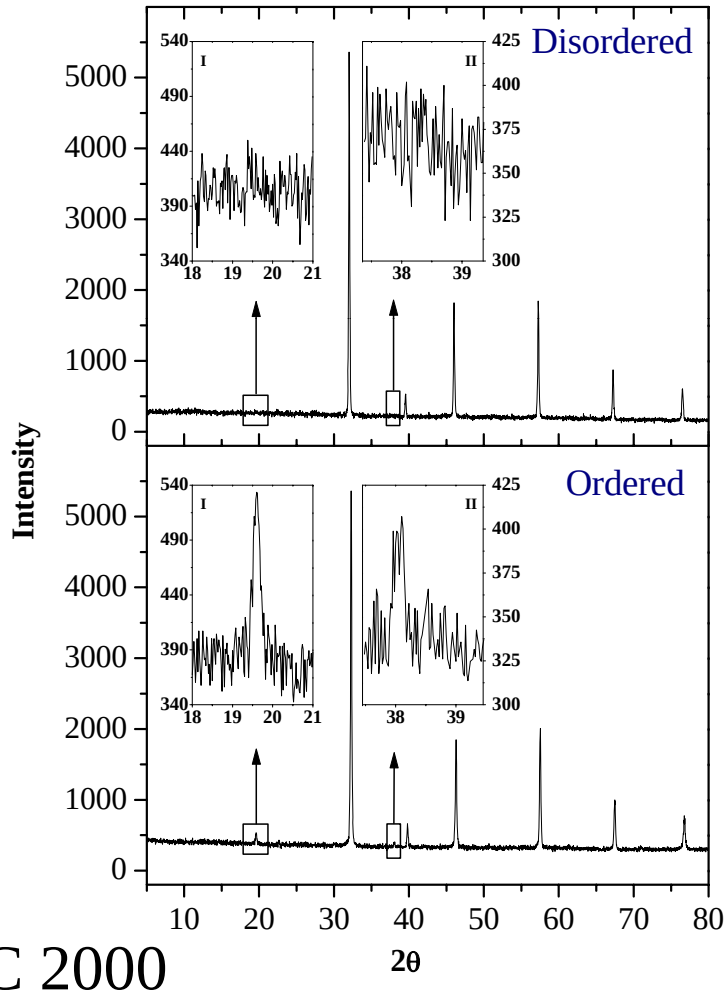

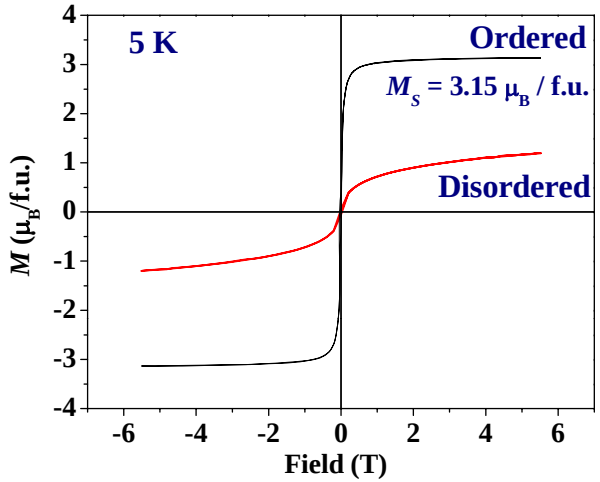

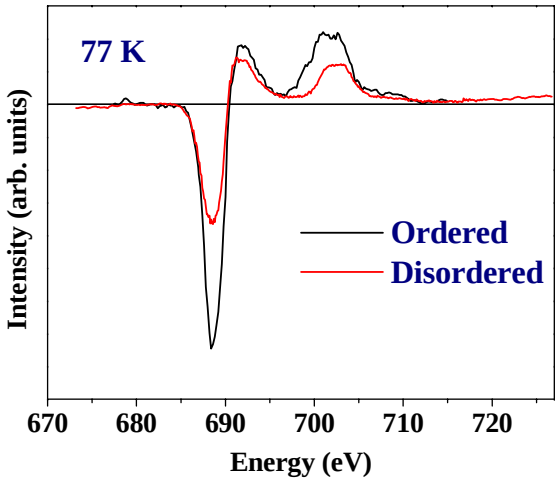

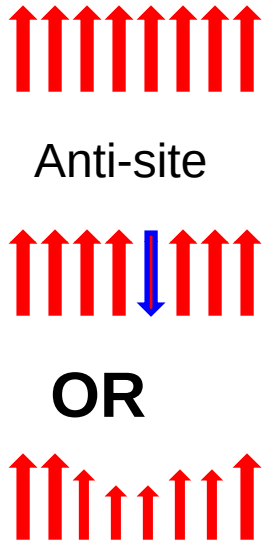

SSC 2000

Why does the magnetisation change so drastically? Fe ↑↓ or Mo d depolarisation?

Does anti-site give rise to antiferromagnetically coupled Fe-O-Fe pairs

OR

Is it depolarisation of Mo bands leading to decoupling of Fe's?

$Sr_2Fe_{1-x}Mo_{1+x}O_6$ $Sr_2Fe_{1+x}Mo_{1-x}O_6$

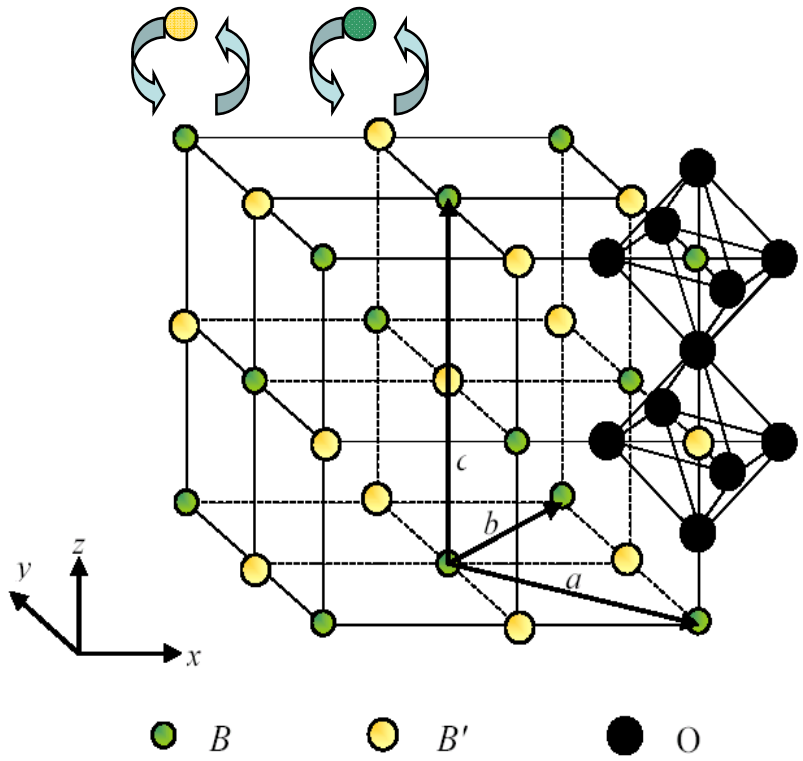

Figure 4 BL10043 18Jan2006

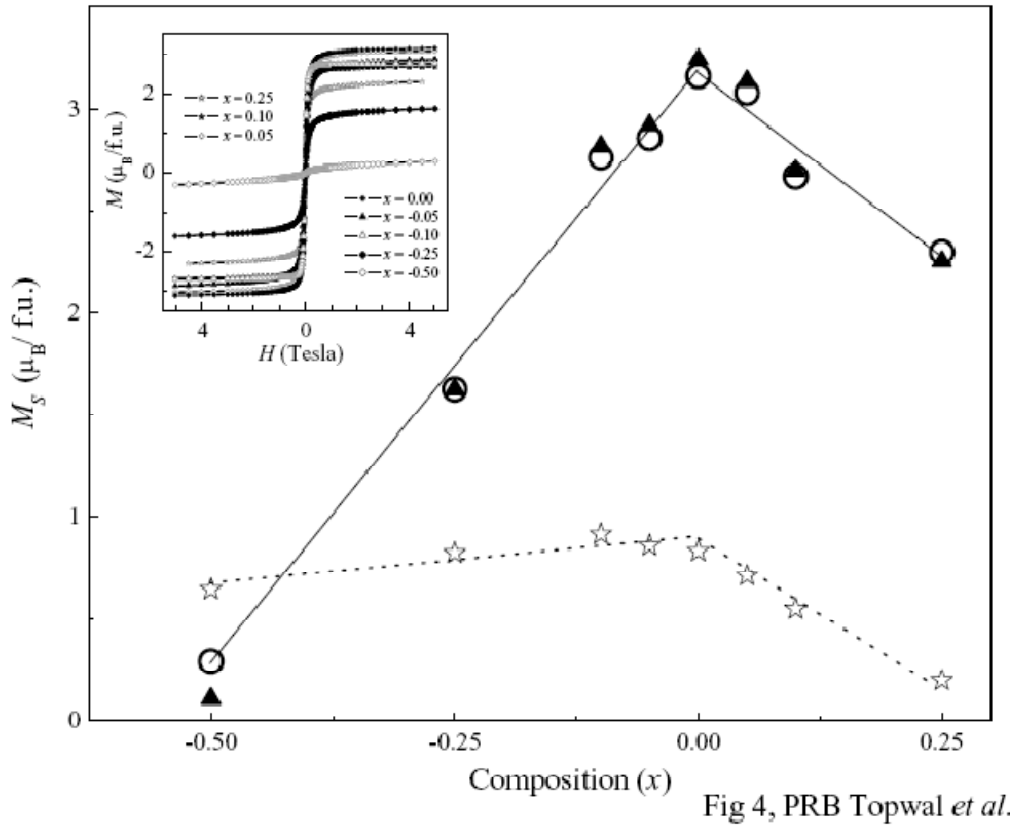

Fig 4, PRB Topwal *et al.*

Nearest neighbour Fe-Fe pairs couple antiferromagnetically and Mo 4d depolarisation.

Magnetoresistance in polycrystalline Sr_2FeMoO_6

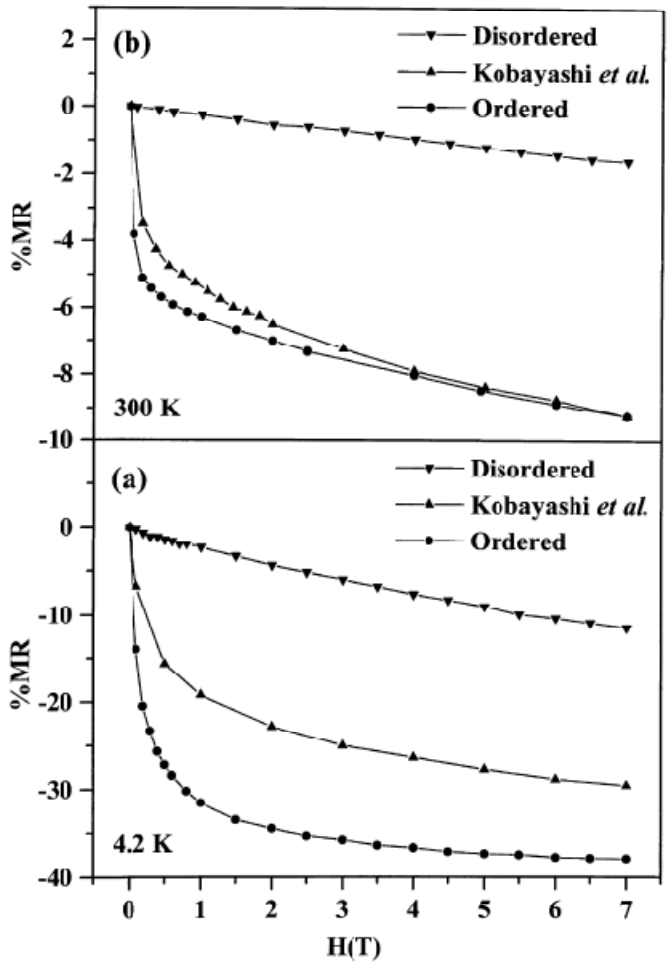

Sarma et al., Solid State Comm. 114, 465 (2000).

But, why does magnetoresistance change so drastically?
Inter- or intra-grain mechanism?

Effect of anti-site disorder in Sr_2FeMoO_6

What is the Fe/Mo antisite disorder?

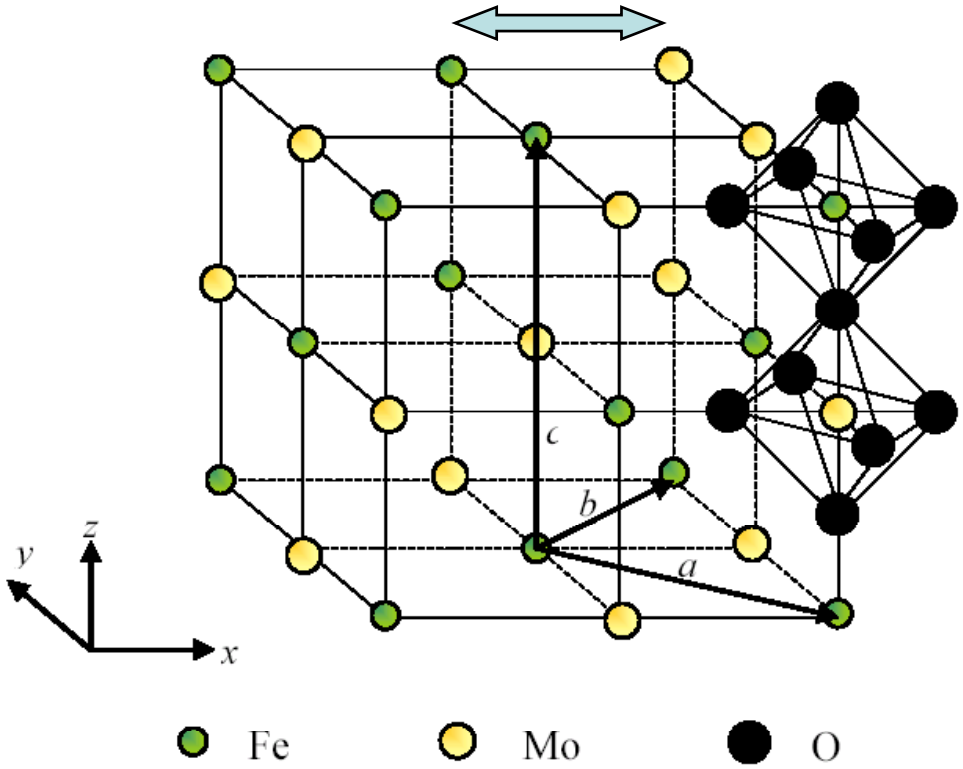

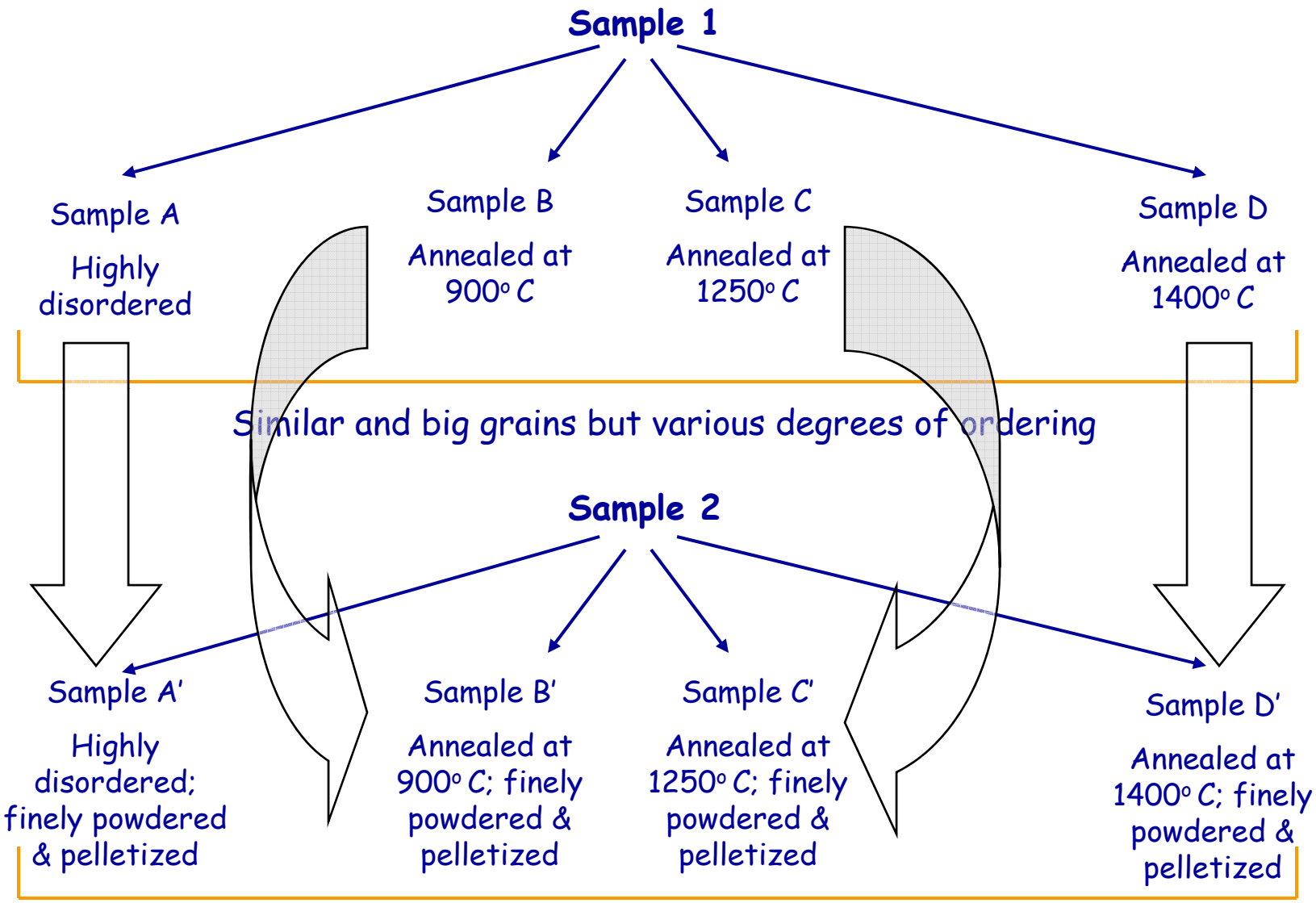
Sample 1
Sample A
Highly disordered
Sample B
Annealed at 900° C
Sample C
Annealed at 1250° C
Sample D
Annealed at 1400° C
Similar and big grains but various degrees of ordering
Sample 2
Sample A'
Highly disordered; finely powdered & pelletized
Sample B'
Annealed at 900° C; finely powdered & pelletized
Sample C'
Annealed at 1250° C; finely powdered & pelletized
Sample D'
Annealed at 1400° C; finely powdered & pelletized
Similar and small grains but various degrees of ordering

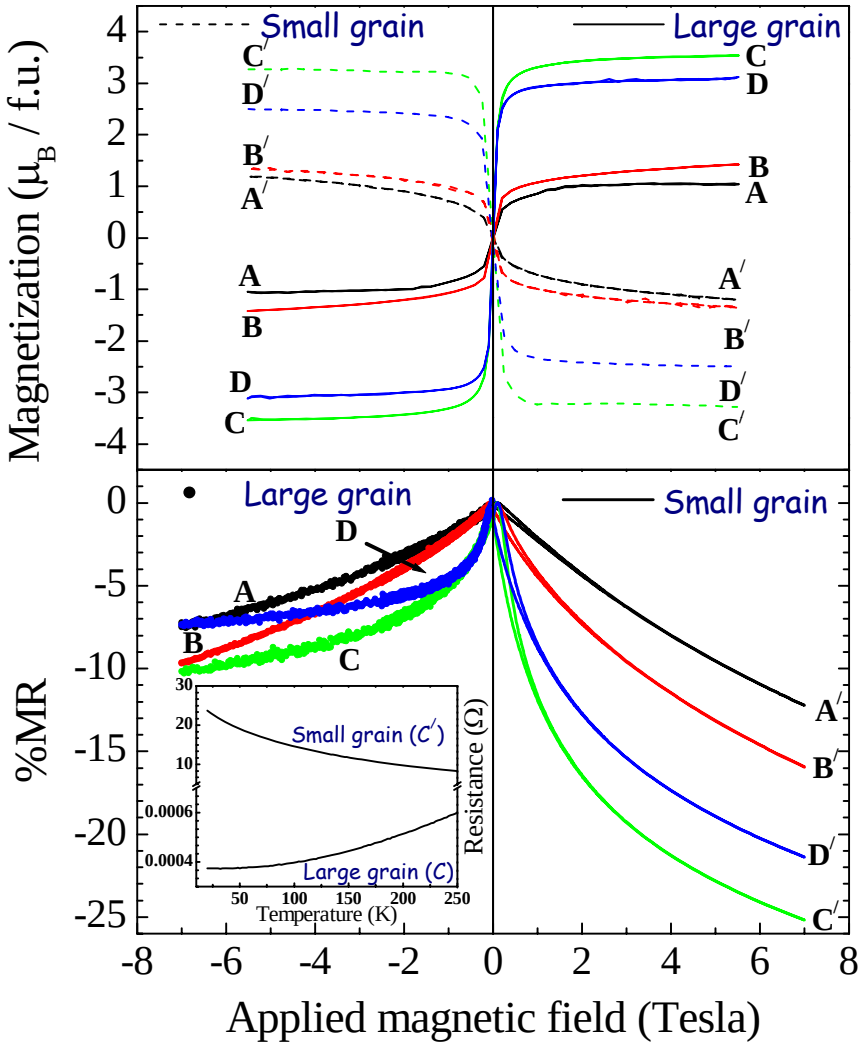

- Small grain samples have much larger %MR compared to the large grain ones → Inter-grain mechanism.
- Within the small grain samples, samples with higher ordering and therefore, lower anti-site defects show larger %MR → Effect of anti-site (intra-grain) boundaries, if any, is dominated over by other (inter-grain and magnetisation) effects.
- Inter-grain tunnelling MR should have some tell-tale signatures, such as %MR ~ M^2 and consistent hysteresis.

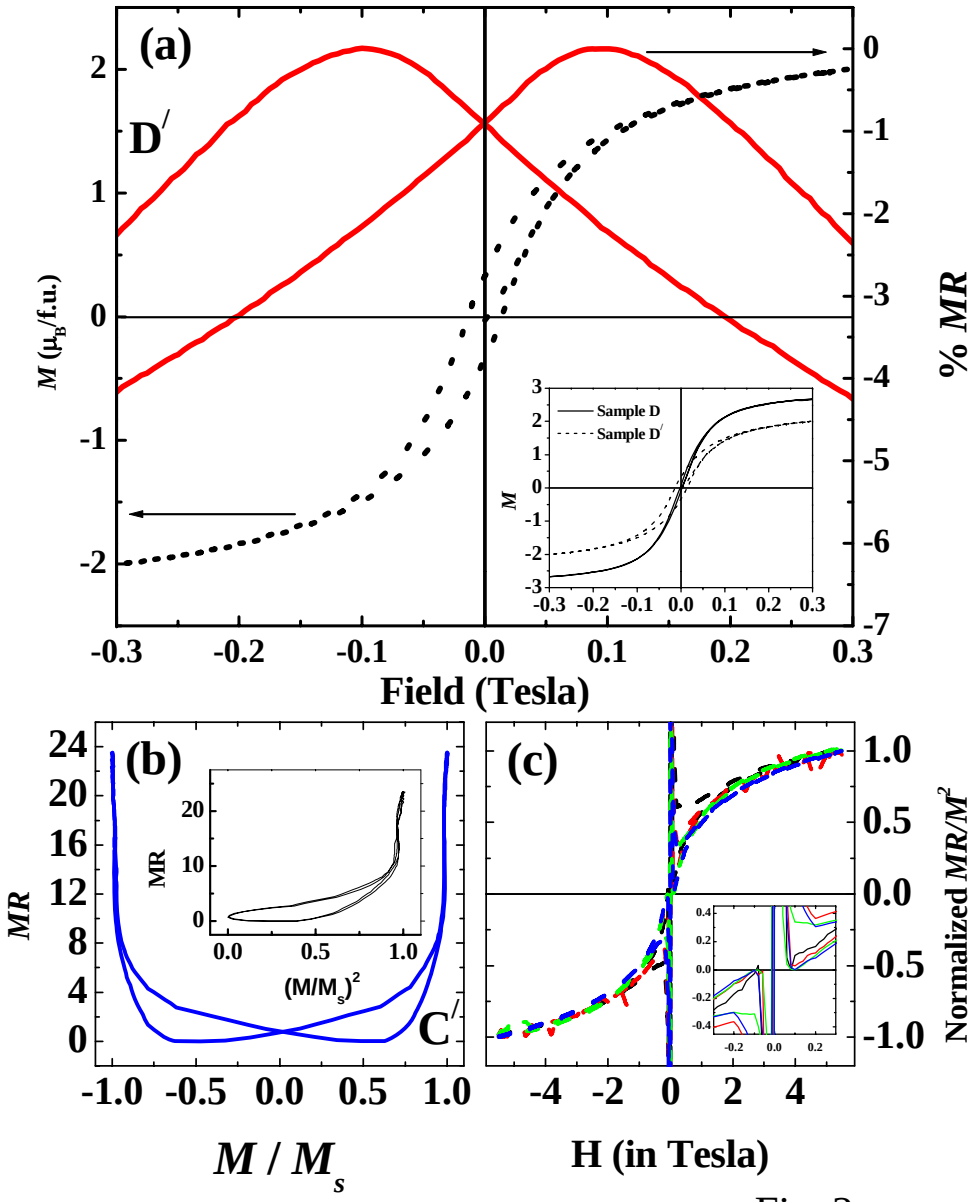

Fig. 2
Sarma *et al.*

TRILAYER MAGNETIC TUNNEL JUNCTION

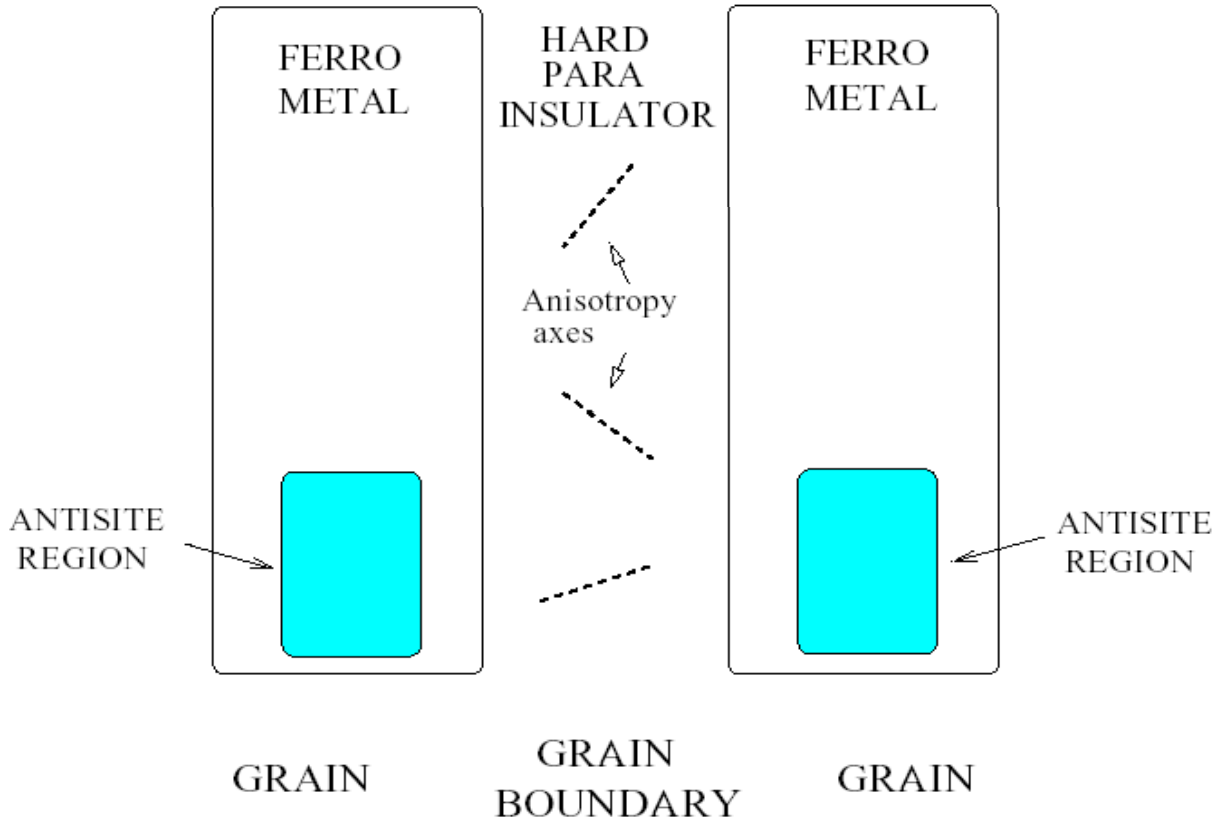

- **Unlike standard TMR calculations, we consider the intermediate insulating region to have magnetic properties also.**

- **The insulating region, in addition to being paramagnetic, is assumed to have magnetic anisotropy, with randomly oriented anisotropy axes.**

Calculated results for MR

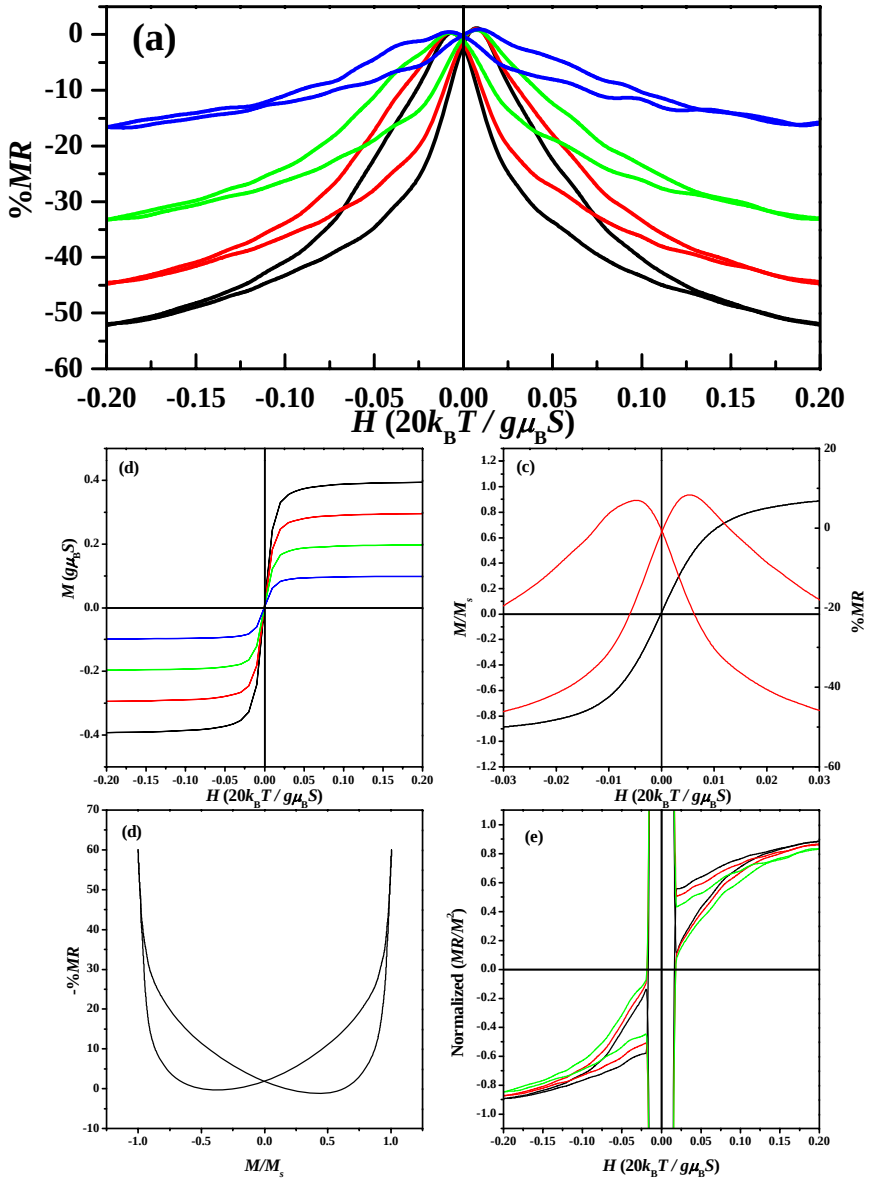

Fig. 3

Effect of anti-site disorder in Sr_2FeMoO_6

What happens if there are several anti-site deffects?

Distributed?

Clustered?

Segregation in 1-d or 2-d?

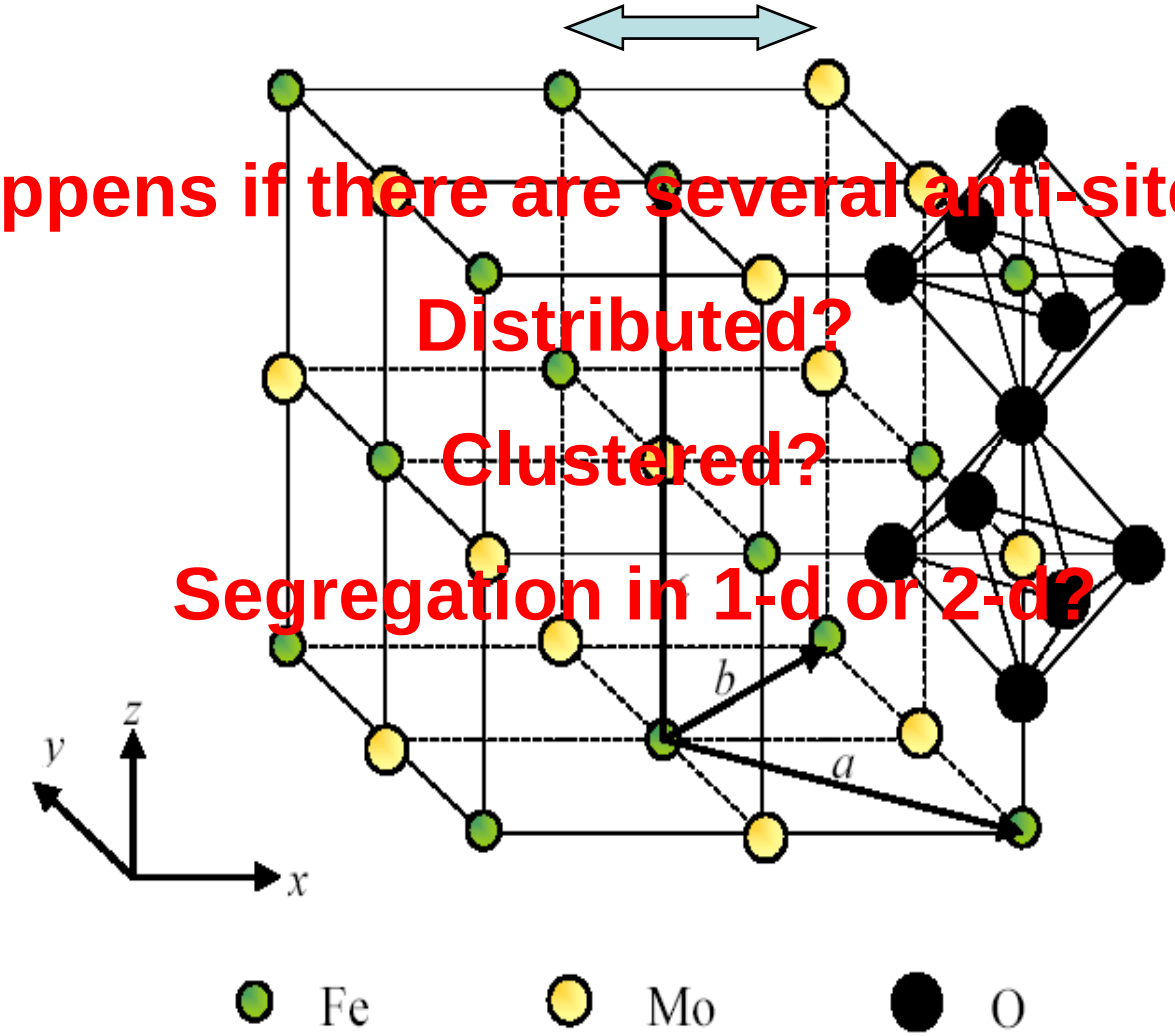

Experimental:

GILDA-BM08 @ ESRF

SR-XRD and XAFS

(Fe & Mo K edges) on Sr_2FeMoO_6 with different cation disorder (S)

XRD

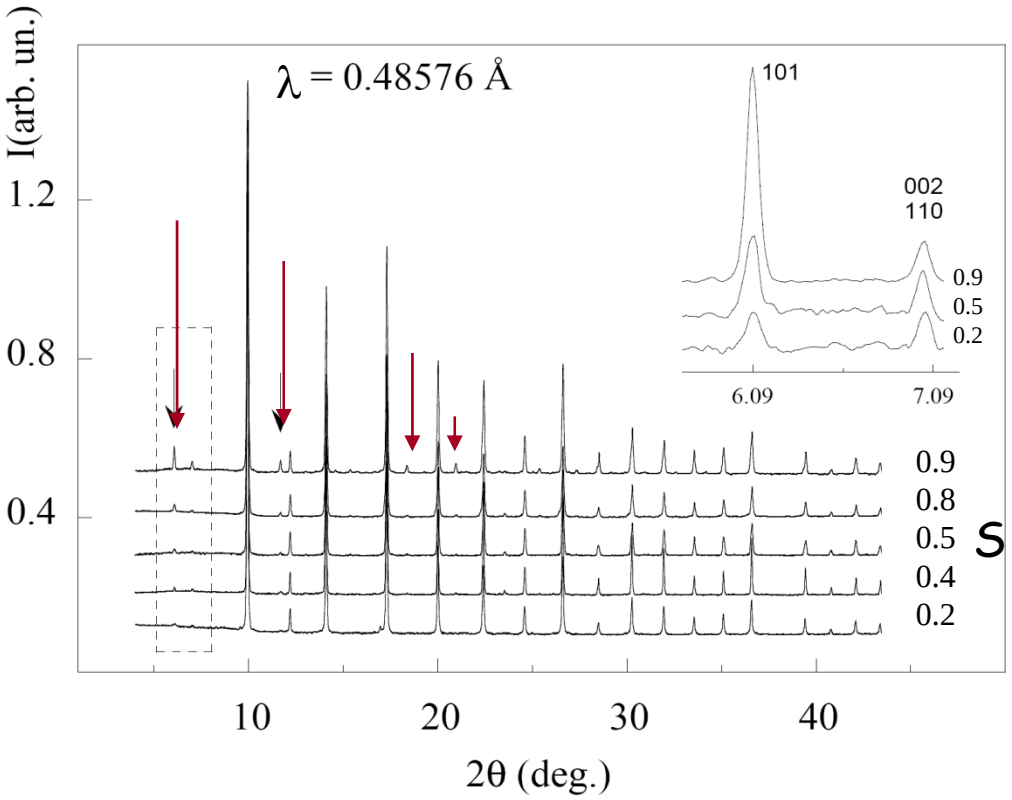

XAFS

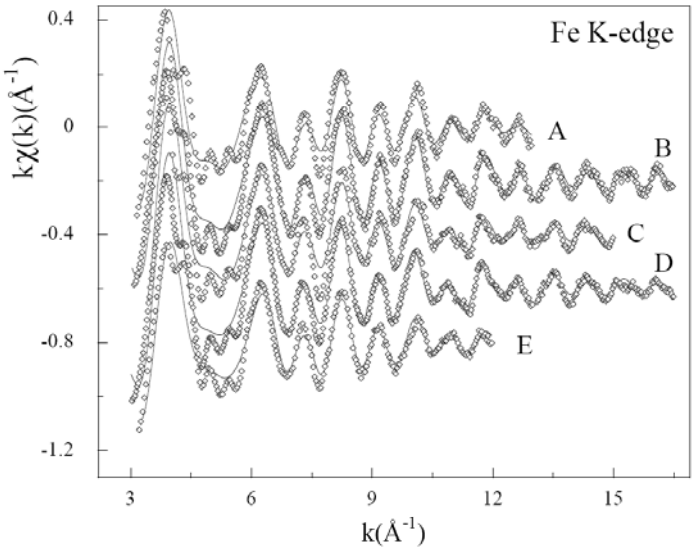

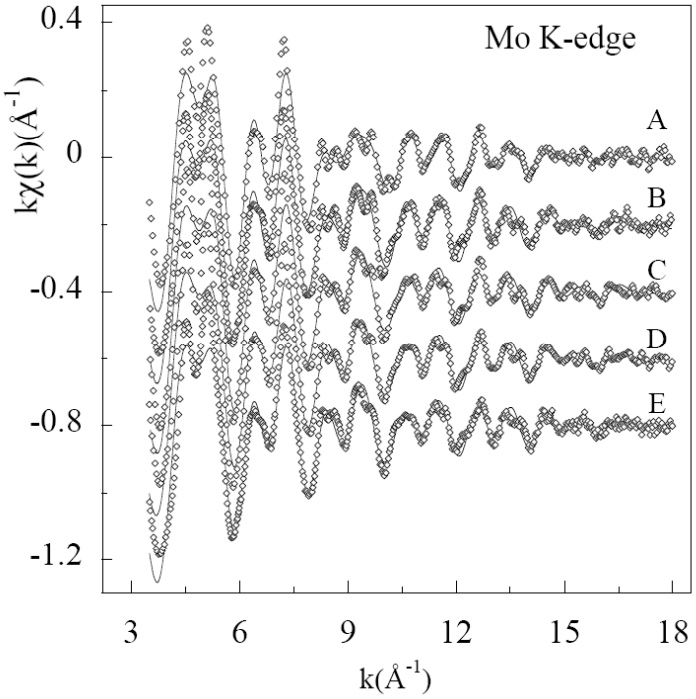

The disorder from a local perspective

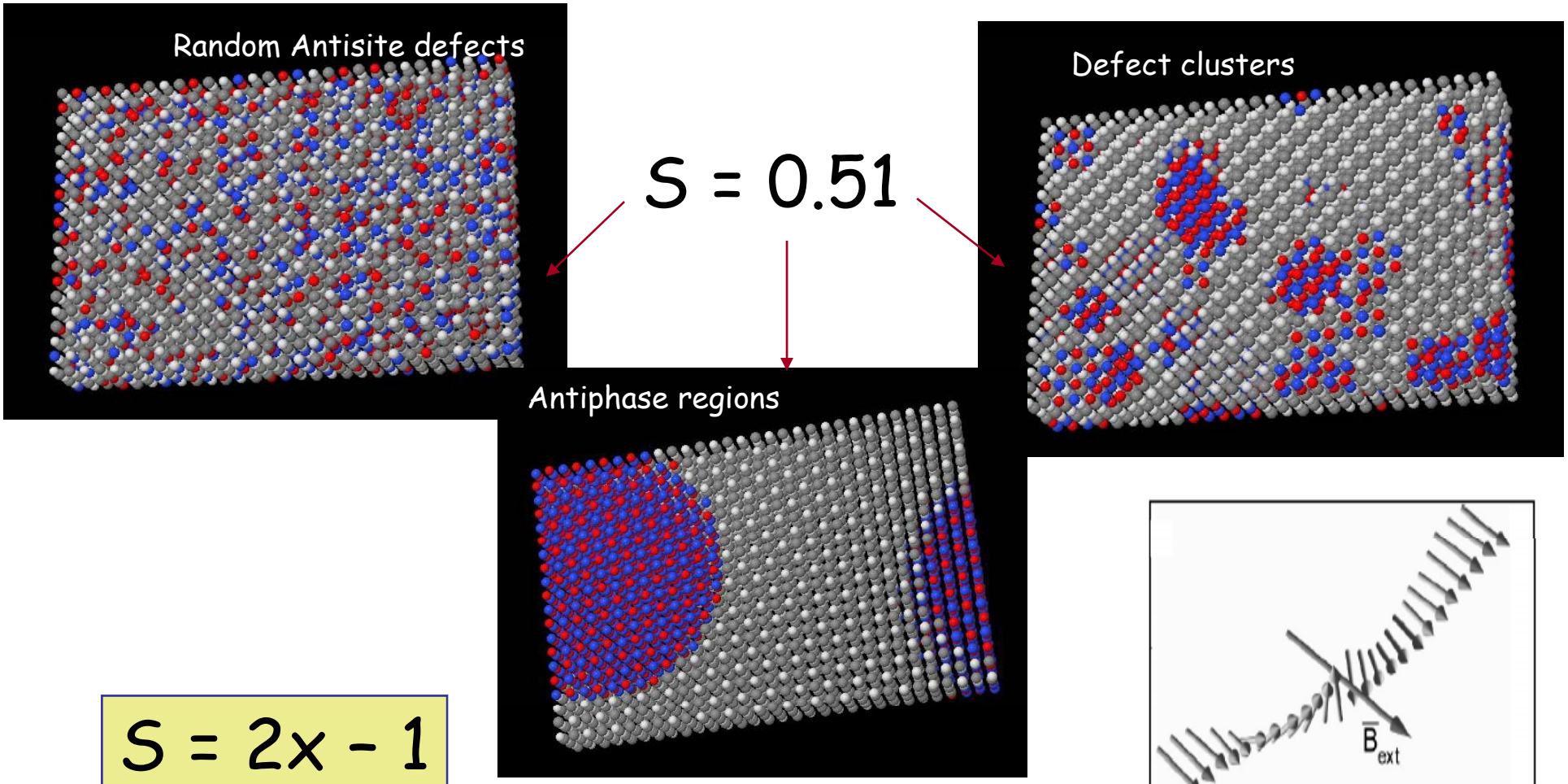

$S = 2x - 1$

S takes into account only for the number of defects (Fe_B or Mo_A), not their arrangement

The nature of defects must affect the magnetic and magnetotransport response of the system

$Sr_2FeMo_xW_{1-x}O_6$

Sr_2FeMoO_6 : Half metallic ferromagnetic metal (T_C ~ 420 K)

Nominally Fe^{3+} and Mo^{5+}.

Sr_2FeWO_6 : Antiferromagnetic insulator (T_N ~ 37 K); Nominally Fe^{2+} localized moments are coupled *via* superexchange through nonmagnetic O^{2-} and W^{6+} sites.

Therefore, $Sr_2FeMo_xW_{1-x}O_6$ assures magnetic and metal-insulator transition over the composition range.

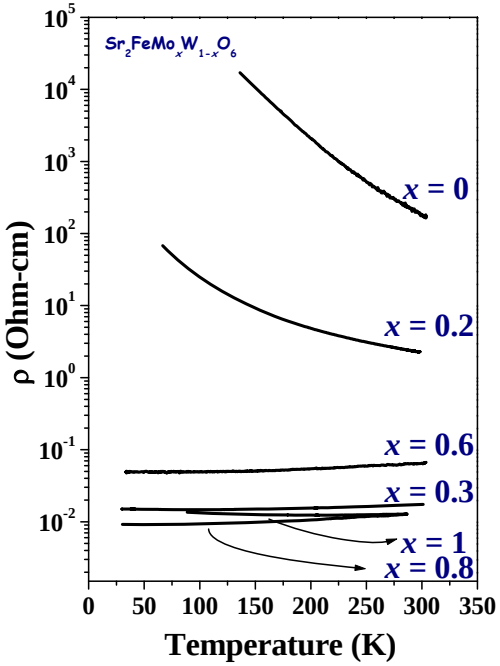

What drives this MIT?

S. Ray et al., J. Physics: Condensed Matter **13**, 607 (2001).

T-*x* Phase diagram of $Sr_2FeMo_xW_{1-x}O_6$

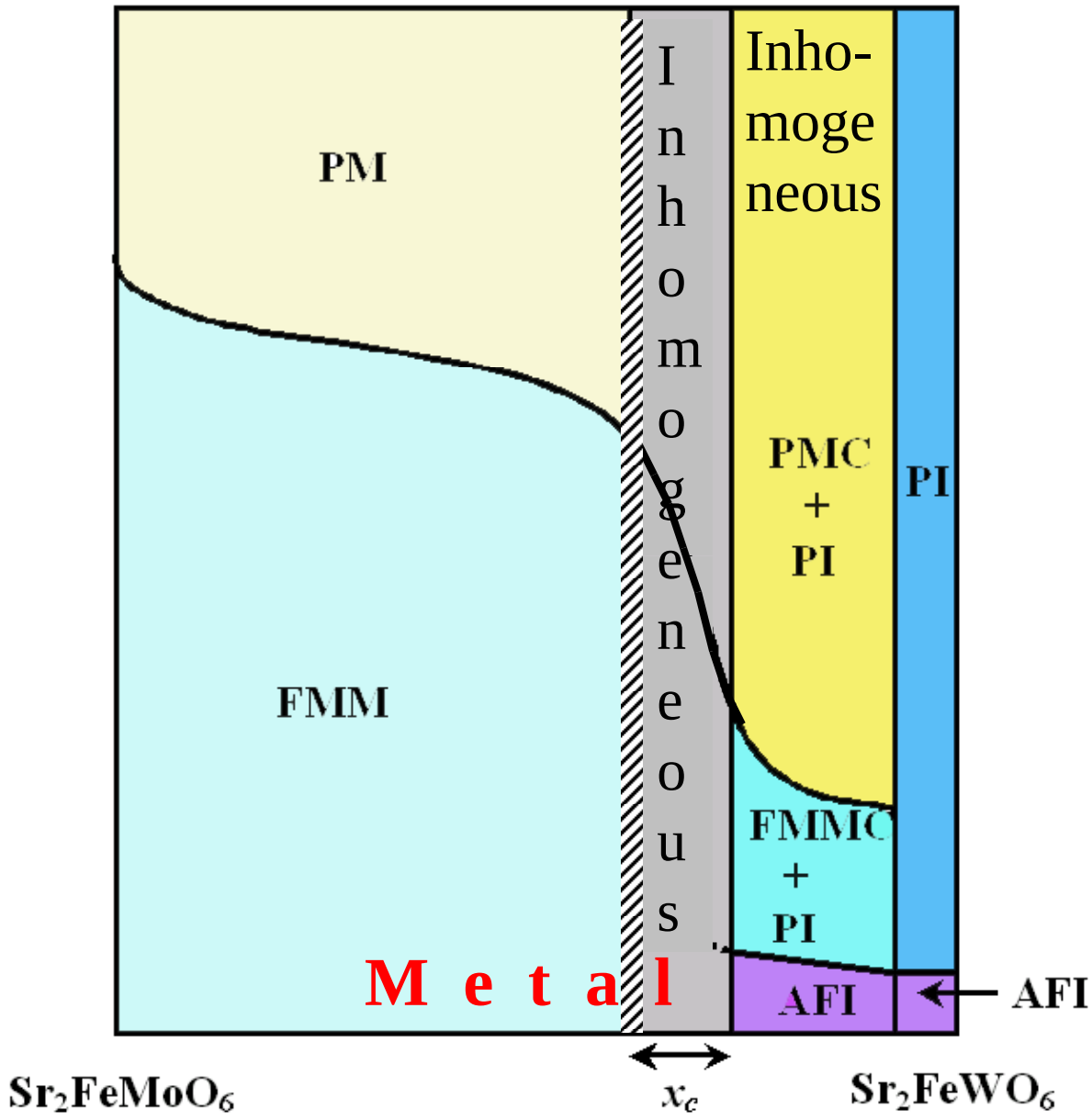

Ray et al., unpublished

Applications of XAFS: Manganites

Temperature dependence of non-Debye disorder in doped manganites

C. Meneghini, R. Cimino, S. Pascarelli, S. Mobilio, C. Raghu and D. D. Sarma

PHYSICAL REVIEW B VOLUME 56, 3520, 1997

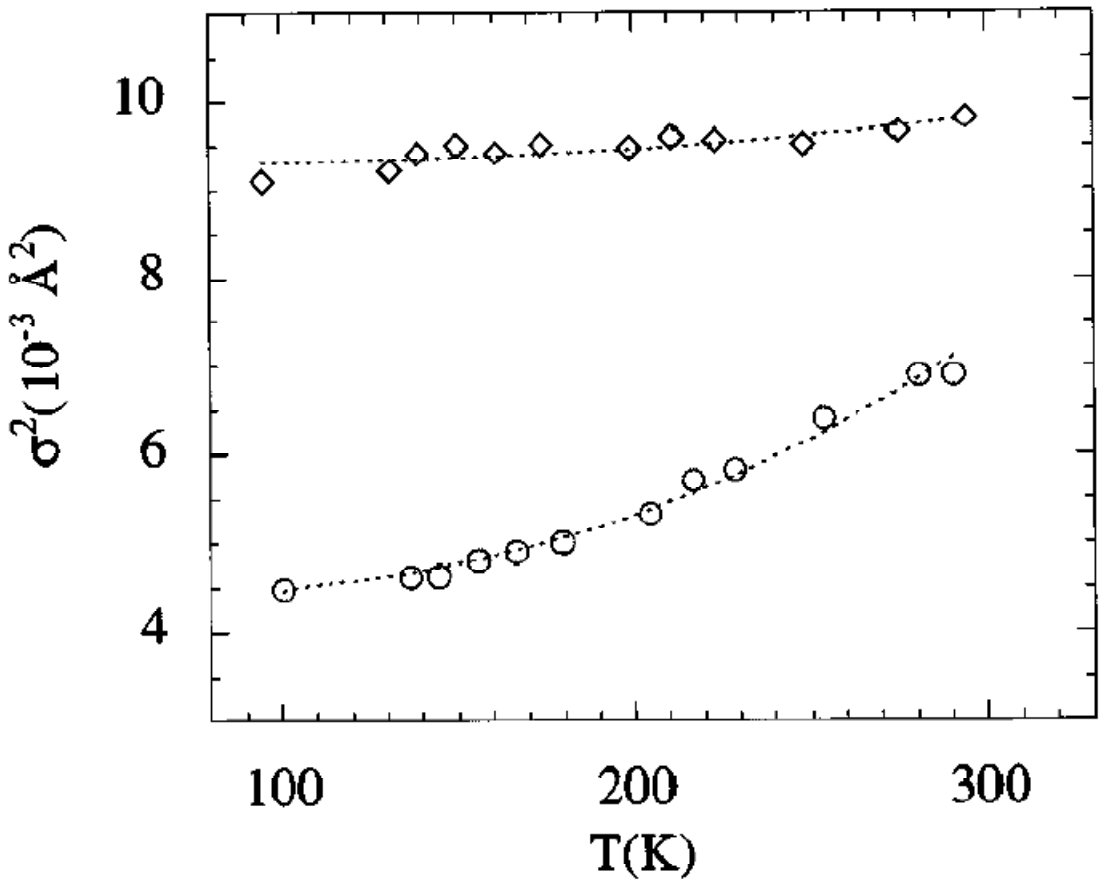

FIG. 1. Debye-Waller factor from EXAFS analysis for $LaMnO_3$ (diamonds) and MnO (circles) samples. The dashed lines are the best fit data obtained using a correlated Debye model (see text).

Meneghini et al., PRB **56** (1997) 3520

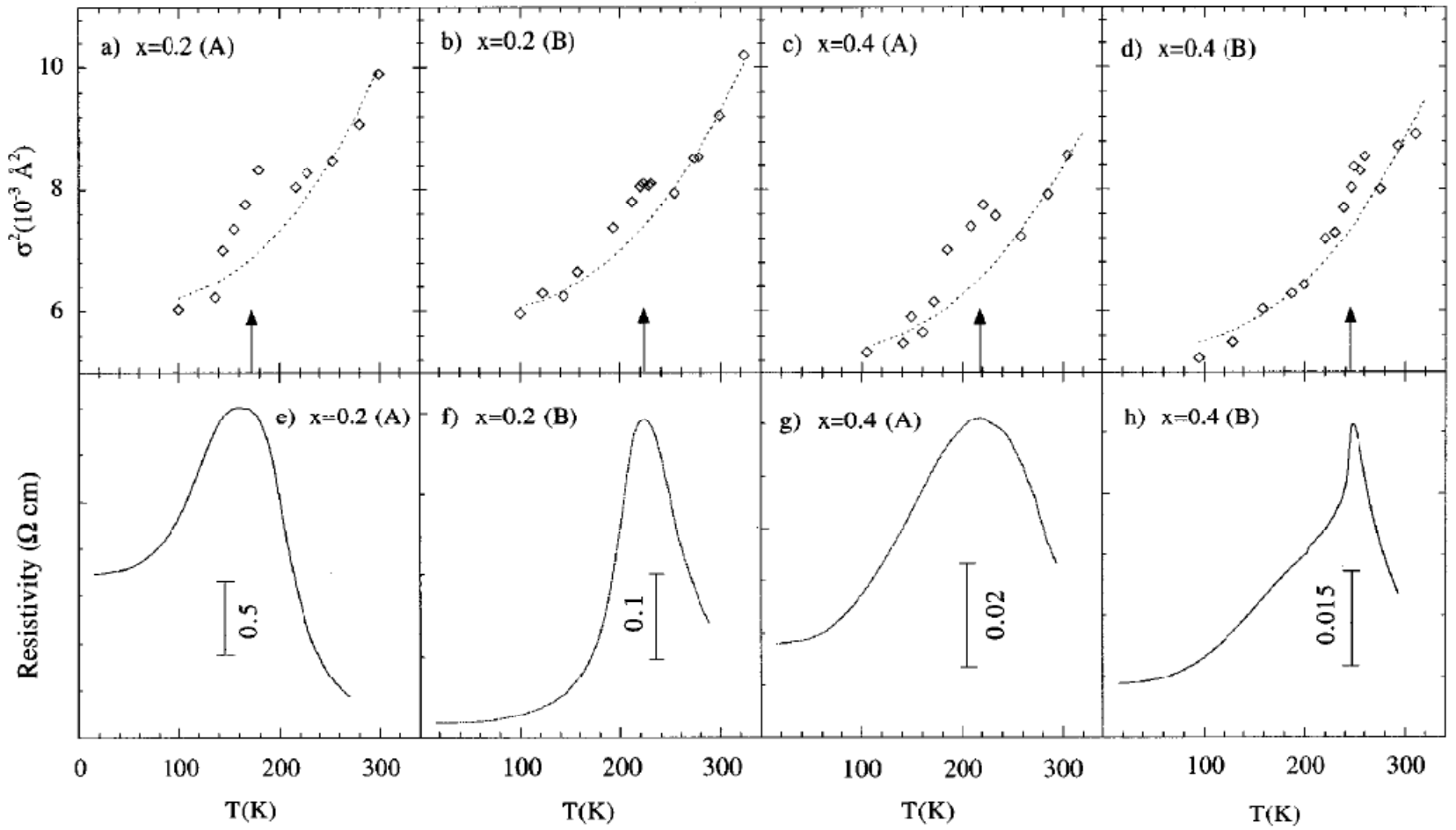

FIG. 2. Top panels (a)–(d): Debye-Waller disorder factor (diamonds) for Ca-doped $La_{1-x}MnO_3Ca_x$ manganites. The arrows indicate the metal-insulator transition temperature and the dashed lines are the Debye-like contribution to the total disorder factor (see text). Bottom panels (e)–(h): resistivity data.

Meneghini et al., PRB **56** (1997) 3520

Local structure of hole-doped manganites: influence of temperature and applied magnetic field.

C. Meneghini, C Castellano, S Mobili , Ashwani Kumar, S Ray and D D Sarma

J. Phys.: Condens. Matter **14** (2002) 1967–1974

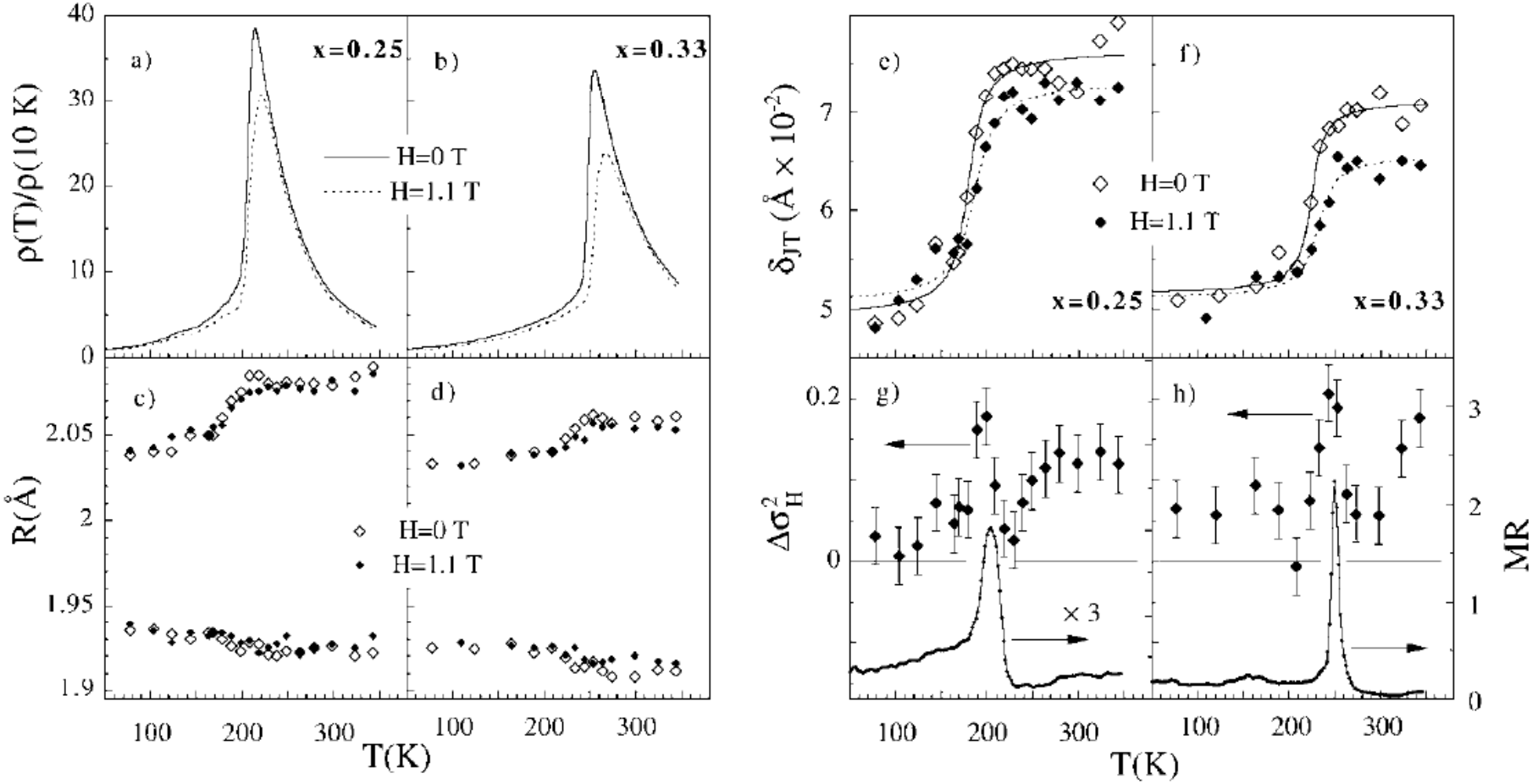

Figure 3. (*a*), (*b*) Resistivity, (*c*), (*d*) bimodal distribution of Mn–O bond lengths and (*e*), (*f*) local Jahn–Teller distortions of the MnO_6 octahedron in the absence ($H = 0$ T) and presence ($H = 1.1$ T) of magnetic field as a function of temperature. In panels (*g*) and (*h*), the relative variations in the DW factors ($\Delta\sigma_H^2 = (\sigma_H^2 - \sigma_0^2)/\sigma_H^2$) and magnetoresistance ($MR = (R_H - R_0)/R_H$) as a function of temperature are shown. Panels (*a*), (*c*), (*e*) and (*g*) ((*b*), (*d*), (*f*) and (*h*)) refer to the $x = 0.25$ (0.33) sample.

C. Meneghini et al., JPCM **14** (2002) 1967

Thank you for your attention